

On the phenomenology of a non-linear $U(1)_Y$ sector

P. De Fabritiis,^{1,*} P. C. Malta,^{2,†} and J. A. Helayël-Neto^{1,‡}

¹*Centro Brasileiro de Pesquisas Físicas (CBPF),*

Rua Dr Xavier Sigaud 150, Urca, Rio de Janeiro, Brazil, 22290-180

²*R. Antonio Vieira 23, 22010-100, Rio de Janeiro, Brazil*

In this work we perform a non-linear extension of the $U(1)_Y$ sector of the Standard Model leading to novel quartic effective interactions between the neutral gauge bosons. We study the induced non-linear effects through high-energy processes resulting in three photons, namely, Z-boson decay and electron-positron annihilation. We also discuss the scattering of neutral gauge bosons induced at tree level. Available experimental data on these processes do not yield viable lower bounds on the mass parameter $\sqrt{\beta}$, but we estimate that the region $\sqrt{\beta} \lesssim m_Z$ could be excluded with higher statistics in future e^-e^+ colliders operating at or above the Z-pole.

I. INTRODUCTION

The idea of non-linear electromagnetic responses of the vacuum was first suggested by Halpern [1], where he proposed that virtual electron-positron pairs could be at the origin of photon-photon collisions. Soon thereafter, actions with non-linear electrodynamics were introduced by Born and Infeld [2] and also Euler and Heisenberg [3] in the 1930's to deal with the classical problem of the infinite self-energy of a point charge. These extensions, which have been also explored in areas as diverse as black-hole physics and cosmology [4–7], can display interesting features, such as vacuum birefringence and dichroism [8–10], and have very recent developments, cf. refs. [11–13]. Perhaps the most striking prediction of these models is the occurrence of light-by-light scattering already at tree-level, a phenomenon recently observed by the ATLAS collaboration in heavy-ion collisions [14, 15]. The perspective to test effects of non-linear extensions of the Standard Model (SM) in high-energy experiments – in lepton and hadron accelerators or potentially in photon-photon colliders – motivates us to search for possible phenomenological consequences.

The non-linear extension of traditional Maxwell electrodynamics modifies photon-photon interactions by introducing higher-order terms in the Lagrangian. Here, we are interested in extending the whole hypercharge sector of the electroweak gauge group, thus giving rise to other interesting phenomena. In fact, besides reproducing the already known non-linear effects in standard electrodynamics (corrected by a factor involving the Weinberg angle), this extension induces anomalous quartic couplings between the Z-boson and the photon. This in turn theoretically allows for rare processes to take place already at tree-level, as for example the creation of a Z-boson pair from the collision of two photons.

There is also a more recent motivation for considering non-linear models. Introduced by Dirac 90 years ago [16], magnetic monopoles remain elusive despite the experimental efforts. It was thought for a long time that it would be impossible to obtain a monopole solution in the electroweak sector because of its gauge structure after symmetry breaking, but this belief turned out to be wrong. An electroweak monopole solution was obtained by Cho and Maison [17], but the original solution predicted an infinite mass that should be regularized to have physical meaning and sustain any hope of being found experimentally. A few years ago, some proposals of SM extensions regularizing the monopole energy and giving a finite, calculable mass were made [18–20]. A non-linear extension of the hypercharge sector could solve the infinite-energy problem, see ref. [21]; a more general extension of the $U(1)_Y$ sector giving a finite-energy monopole solution was investigated in ref. [22]. Nowadays there is hope to finally find a monopole in the MoEDAL experiment [23], for example, and it is important to understand what are the phenomenological implications of such an extension.

Non-linear effects have not been observed at low energies. This means that the parameter controlling the non-linearity of the fields is expected to be large in comparison to other relevant energy scales. The parameters in non-linear theories may be constrained in different ways, *e.g.*, via hydrogen spectroscopy or interferometry [24, 25]. The state-of-the-art bound is obtained in ref. [26] using recent LHC data on light-by-light scattering in heavy-ion collisions. The lower bound reported there, “under quite conservative assumptions”, is ~ 100 GeV, but it could reach ~ 200 GeV under less restrictive assumptions. As a matter of fact, this mass parameter may reach the TeV scale (or even higher) in brane-inspired models.

In this work we analyse an extension of the hypercharge sector of the SM. This gives rise to quartic effective interactions between the neutral gauge bosons absent in the SM at tree level. These novel operators contribute to decay and scattering processes and we explore existing experimental data to place lower bounds on the non-linear parameter. Furthermore, we briefly discuss possible improvements on the bounds in future experiments.

* pdf321@cbpf.br

† pedrocmalta@gmail.com

‡ helayel@cbpf.br

This paper is organized as follows: in sec. II we present the theoretical setup of our model. In sec. III we discuss options to constrain the expansion parameter β , in particular through the decay $Z \rightarrow 3\gamma$ in sec. III A and the scattering $e^- e^+ \rightarrow 3\gamma$ in sec. III B, respectively. In sec. III C we briefly discuss other purely quartic scattering processes that may be relevant in future experiments. Finally, in sec. IV we present our closing remarks. We use natural units ($c = \hbar = 1$) and the flat Minkowski metric $\eta^{\mu\nu} = \text{diag}(+1, -1, -1, -1)$ throughout.

II. THEORETICAL SETUP

Let us briefly review the usual electroweak (EW) Lagrangian to fix our notation. The bosonic part of the EW sector is given by

$$\mathcal{L}_{\text{EW}} = \mathcal{L}_{\text{Gauge}} + \mathcal{L}_{\text{Higgs}}, \quad (1)$$

where

$$\mathcal{L}_{\text{Gauge}} = -\frac{1}{4}F_{\mu\nu}^a F_{\mu\nu}^a - \frac{1}{4}B_{\mu\nu}B_{\mu\nu}, \quad (2)$$

$$\mathcal{L}_{\text{Higgs}} = |D_\mu H|^2 - \lambda \left(H^\dagger H - \frac{m^2}{2\lambda} \right)^2. \quad (3)$$

Here we defined the covariant derivative as

$$D_\mu = \partial_\mu - igA_\mu^a T^a - ig'Y B_\mu. \quad (4)$$

In the equations above, A_μ^a and B_μ are the gauge fields associated with the gauge group $SU(2)_L \times U(1)_Y$, $F_{\mu\nu}^a = \partial_\mu A_\nu^a - \partial_\nu A_\mu^a + g\epsilon_{abc}A_\mu^b A_\nu^c$ and $B_{\mu\nu} = \partial_\mu B_\nu - \partial_\nu B_\mu$ are the respective field strengths, g and g' are the couplings. Here T^a are the generators of $SU(2)_L$ satisfying $[T^a, T^b] = i\epsilon^{abc}T^c$ and Y is the weak hypercharge.

The Higgs field H is a $SU(2)_L$ doublet with hypercharge $Y(H) = +1/2$. The scalar potential induces a non-trivial vacuum expectation value given by $|\langle H \rangle|^2 = v^2/2 = m^2/2\lambda$. Below this energy scale, the theory is cast into the Higgs phase with three massive vector bosons W^\pm, Z , a massive scalar h and a massless photon A (γ) in the spectrum. The physical fields can be written using the Weinberg angle θ_W : the neutral vector bosons are defined by $Z_\mu = \cos\theta_W A_\mu^3 - \sin\theta_W B_\mu$ and $A_\mu = \sin\theta_W A_\mu^3 + \cos\theta_W B_\mu$, whereas the charged vector fields are defined by $W_\mu^\pm = (A_\mu^1 \mp iA_\mu^2)/\sqrt{2}$.

The masses of the vector bosons can be precisely measured and are $m_W = gv/2 = 80.4$ GeV and $m_Z = m_W/\cos\theta_W = 91.2$ GeV. The Weinberg angle can be experimentally determined and satisfies $\sin^2\theta_W = 0.23$. After symmetry breaking, the kinetic part of the gauge Lagrangian (omitting mass terms) reads

$$\mathcal{L}_{\text{Gauge}}^{\text{Kin}} = -\frac{1}{4}F_{\mu\nu}F^{\mu\nu} - \frac{1}{4}Z_{\mu\nu}Z^{\mu\nu} - \frac{1}{2}W_{\mu\nu}^+W^{\mu\nu-}, \quad (5)$$

where the field-strength tensors are defined as usual.

We may now introduce the leptons through the following Lagrangian:

$$\mathcal{L}_{\text{Leptons}} = i\bar{L}_i\gamma^\mu D_\mu L_i + i\bar{\ell}_{iR}\gamma^\mu D_\mu \ell_{iR}, \quad (6)$$

where L_i denotes the lepton doublets $L_i = (\nu_{iL} \ell_{iL})^t$ with ν_{iL} , ℓ_{iL} and ℓ_{iR} representing the left-handed neutrinos, the left-handed charged leptons and the right-handed lepton fields, respectively. Here i is a flavor index to distinguish between the three generations of leptons. The hypercharge assignment adopted here is: $Y(L_i) = -1/2$ and $Y(\ell_{iR}) = -1$. Taking eq. (6) with eq. (4) including the gauge fields after symmetry breaking we obtain the interactions between matter and gauge fields. In what follows only two such interaction terms will be relevant, namely,

$$\mathcal{L}_{ee\gamma} = -e\bar{\ell}_i\gamma_\mu \ell_i A^\mu, \quad (7)$$

$$\mathcal{L}_{eeZ} = \frac{g}{4\cos\theta_W}\bar{\ell}_i\gamma_\mu (-1 + 4\sin^2\theta_W + \gamma^5)\ell_i Z^\mu. \quad (8)$$

Here we propose the following general extension of the weak hypercharge sector of the EW Lagrangian:

$$\mathcal{L} = -\frac{1}{4}B_{\mu\nu}B^{\mu\nu} \quad \longrightarrow \quad \mathcal{L}_Y = f(\mathcal{F}, \mathcal{G}), \quad (9)$$

where we defined the Lorentz and gauge invariant objects

$$\mathcal{F} = \frac{1}{4}B_{\mu\nu}B^{\mu\nu} \quad \text{and} \quad \mathcal{G} = \frac{1}{4}B_{\mu\nu}\tilde{B}^{\mu\nu} \quad (10)$$

with the dual field-strength tensor given by $\tilde{B}^{\mu\nu} = \frac{1}{2}\epsilon^{\mu\nu\rho\sigma}B_{\rho\sigma}$. This type of non-linear extension was already studied in the context of magnetic monopoles [22], where it was shown that under certain conditions, it allows a finite-energy electroweak monopole solution.

The SM predictions are so far in excellent agreement with experiment and, in order to recover the usual SM results, we demand that our general extension $f(\mathcal{F}, \mathcal{G})$ reproduces the usual term $-\frac{1}{4}B_{\mu\nu}B^{\mu\nu}$ in some appropriate limit. Since we do not want to have a parity-violating term in the photon sector after spontaneous symmetry breaking, we impose the physically motivated assumption that $f(\mathcal{F}, \mathcal{G})$ depends on \mathcal{G} only through \mathcal{G}^2 .

Let us consider for instance a Born-Infeld (BI) extension of the hypercharge sector [2] given by

$$\mathcal{L}_Y^{\text{BI}} = \beta^2 \left[1 - \sqrt{1 + 2 \left(\frac{\mathcal{F}}{\beta^2} - \frac{\mathcal{G}^2}{2\beta^4} \right)} \right], \quad (11)$$

where β is a parameter with dimension of mass squared. This non-linear extension has been extensively studied in the context of electrodynamics, with applications in a range of subjects, and has attracted a lot of interest in the recent years after the observation of light-by-light scattering at the LHC [14, 15]. Interestingly enough, the BI action can be derived from string theory [27] and also appears in the dynamics of D-branes [28].

Our goal is to study the phenomenological consequences of the non-linear extension in high-energy processes. To accomplish this, we need to obtain the induced operators written in terms of the physical fields after symmetry breaking. The mass scale set by $\sqrt{\beta}$ is expected to be large in comparison with the typical energies of the processes considered, motivating us to perform a Taylor expansion of eq. (11) in powers of $X = \frac{\mathcal{F}}{\beta^2} - \frac{\mathcal{G}^2}{2\beta^4}$:

$$\mathcal{L}_Y = -\mathcal{F} + \frac{1}{2\beta^2} [\mathcal{F}^2 + \mathcal{G}^2] + \mathcal{O}(1/\beta^4). \quad (12)$$

We will only consider tree-level processes with at most four gauge bosons in each vertex, so we can safely restrict ourselves to leading non-trivial order. It is important to keep in mind that this perturbative approach can only be trusted as long as the energy of the process is lower than the mass scale set by $\sqrt{\beta}$, as this guarantees that the next terms in the expansion provide increasingly negligible corrections to the leading-order terms.

Furthermore, taking into consideration the recent interest in different versions of non-linear electrodynamics, we can also consider other interesting extensions that would give rise to the same physical effects in the approximation considered here. In fact, using X defined above, we could as well have considered here the extensions given by $\mathcal{L}_Y^{\text{Log}} = -\beta^2 \log[1 + X]$ and $\mathcal{L}_Y^{\text{Exp}} = \beta^2 [e^{-X} - 1]$ giving us the $U(1)_Y$ version of the logarithmic [8] and exponential [9, 10] non-linear electrodynamics. The three extensions agree up to leading non-trivial order and we will restrict ourselves to tree-level processes with at most four gauge bosons interactions, so we may safely consider the β parameters as being equal with a good approximation and use eq. (12) to describe their common effects.

The Lagrangian above is a function of the $U(1)_Y$ gauge field, B_μ , but after symmetry breaking we can write it in terms of the physical fields, A_μ and Z_μ , retrieving the usual SM kinetic terms at zeroth order. At first order we have ($s_\theta \equiv \sin \theta_W$, $c_\theta \equiv \cos \theta_W$)

$$\begin{aligned} \mathcal{L}_Y^{(1/\beta^2)} = & \frac{1}{32\beta^2} \left\{ s_\theta^4 \left[(ZZ)(ZZ) + (Z\tilde{Z})(Z\tilde{Z}) \right] \right. \\ & + c_\theta^4 \left[(FF)(FF) + (F\tilde{F})(F\tilde{F}) \right] \\ & + 2s_\theta^2 c_\theta^2 \left[(FF)(ZZ) + (F\tilde{F})(Z\tilde{Z}) \right] \\ & + 4s_\theta^2 c_\theta^2 \left[(ZF)(ZF) + (Z\tilde{F})(Z\tilde{F}) \right] \\ & - 4s_\theta^3 c_\theta \left[(ZZ)(ZF) + (Z\tilde{Z})(Z\tilde{F}) \right] \\ & \left. - 4s_\theta c_\theta^3 \left[(FF)(FZ) + (F\tilde{F})(F\tilde{Z}) \right] \right\}, \quad (13) \end{aligned}$$

where we defined $(ZZ) \equiv Z_{\mu\nu} Z^{\mu\nu}$ with an analogous definition for the dual versions. All non-linearly induced vertices above have the same momentum structure and very similar Feynman rules; this traces back to the common origin of such interactions.

In conclusion, we see that our non-linear extension in the hypercharge sector generates a series of dimension-eight effective operators generically suppressed by a factor $(\mathcal{E}/\Lambda)^4$, where \mathcal{E} is a typical energy scale characteristic of the process and Λ is the mass scale set by $\sqrt{\beta}$. These effective operators will introduce new vertices, allowing processes that could only occur in the SM at loop level to take place already at tree level. In the next section we explore this fact and consider different high-energy processes to obtain lower bounds on β whenever experimental data are available. We also discuss the impact of our non-linear extension on scattering processes involving neutral gauge bosons.

III. EXPERIMENTAL LIMITS

In the section above we have extracted quartic interaction vertices between the photon and Z-boson which are completely absent from the SM, thus opening up interesting possibilities to constrain the expansion parameter β . In the following we explore a few of them.

A. $Z \rightarrow 3\gamma$

In the SM there is no tree-level $Z\gamma\gamma\gamma$ vertex, so the decay process $Z \rightarrow 3\gamma$ proceeds exclusively via fermion and W-boson loops [32, 33]. The theoretical prediction for the partial width is $\Gamma(Z \rightarrow 3\gamma)_{\text{SM}} = 1.4 \text{ eV}$ [34] and, given the experimentally determined total width of the Z-boson $\Gamma_{\text{exp}}^Z = 2.49 \text{ GeV}$ [35], the expected branching ratio is $\text{BR}(Z \rightarrow 3\gamma)_{\text{SM}} = 5.4 \times 10^{-10}$. The currently best upper bound was obtained by the ATLAS collaboration using pp collisions at $\sqrt{s} = 8 \text{ TeV}$ and reads [36]

$$\text{BR}(Z \rightarrow 3\gamma)_{\text{exp}} < 2.2 \times 10^{-6}, \quad (14)$$

representing a five-fold improvement on the previous determination from LEP [37]. This process is clearly very rare and could not yet be measured directly. It is thus an ideal testing ground for new physics [38, 39].

The SM prediction is compatible with the best current experimental bound, but there is a vast gap between them. The non-linear extension can therefore be constrained by comparing its prediction to the experimental bound, cf. eq. (14). The tree-level amplitude for a Z-boson with 4-momentum p decaying into three photons with 4-momenta q_k ($k = 1, 2, 3$) is (cf. fig. 1)

$$-i\mathcal{M} = \epsilon_\alpha(p) V_{Z3\gamma}^{\alpha\beta\gamma\delta}(\beta) \epsilon_\beta^*(q_1) \epsilon_\gamma^*(q_2) \epsilon_\delta^*(q_3), \quad (15)$$

where the vertex factor

$$V_{Z3\gamma}^{\alpha\beta\gamma\delta}(\beta) = -i \frac{s_\theta c_\theta^3}{\beta^2} f^{\alpha\beta\gamma\delta} \quad (16)$$

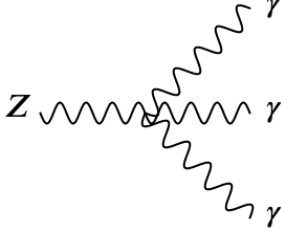


Figure 1. Tree-level Feynman diagram for the decay $Z \rightarrow 3\gamma$.

may be read from the last line of eq. (13). The momentum-dependent function $f^{\alpha\beta\gamma\delta}$ is given by

$$\begin{aligned}
-f^{\alpha\beta\gamma\delta} = & \left[(q_1 \cdot q_2) \eta^{\beta\gamma} - q_1^\gamma q_2^\beta \right] \left[(p \cdot q_3) \eta^{\alpha\delta} - p^\delta q_3^\alpha \right] \\
& + \left[(q_1 \cdot q_3) \eta^{\beta\delta} - q_1^\delta q_3^\beta \right] \left[(p \cdot q_2) \eta^{\alpha\gamma} - p^\gamma q_2^\alpha \right] \\
& + \left[(q_2 \cdot q_3) \eta^{\gamma\delta} - q_2^\delta q_3^\gamma \right] \left[(p \cdot q_1) \eta^{\alpha\beta} - p^\beta q_1^\alpha \right] \\
& + \epsilon^{\mu\beta\rho\gamma} \epsilon^{\nu\delta\kappa\alpha} p_\kappa q_{1\mu} q_{2\rho} q_{3\nu} \\
& + \epsilon^{\mu\beta\rho\delta} \epsilon^{\nu\gamma\kappa\alpha} p_\kappa q_{1\mu} q_{2\nu} q_{3\rho} \\
& + \epsilon^{\mu\gamma\rho\delta} \epsilon^{\nu\beta\kappa\alpha} p_\kappa q_{1\nu} q_{2\mu} q_{3\rho}. \tag{17}
\end{aligned}$$

Here we have assumed that p flows into the vertex, whereas the q_k flow out of it. Incidentally, this momentum structure is the same for all vertices in eq. (13).

From this point on, we neglect the loop-level SM amplitude so the tree-level result from eq. (15) is essentially the only contribution to the decay. The unpolarized squared amplitude reads

$$\langle |\mathcal{M}|^2 \rangle = \frac{8s_\theta^2 c_\theta^6}{3\beta^4} \Phi(p, q_1, q_2, q_3), \tag{18}$$

with the momentum factor given by

$$\Phi(p, q_1, q_2, q_3) = \frac{1}{2} (p \cdot q_1)^2 (q_2 \cdot q_3)^2 + \text{perm.}, \tag{19}$$

where ‘‘perm.’’ indicates all permutations of the q_k . In the rest frame of the decaying Z-boson, $p^\mu = (m_Z, 0)$, and the outgoing photons have $E_k = |\mathbf{q}_k|$. By applying the usual dispersion relations and momentum conservation, we find

$$p \cdot q_3 = m_Z E_3 \quad \text{and} \quad q_1 \cdot q_2 = \frac{m_Z^2}{2} - m_Z E_3, \tag{20}$$

with similar results for the other 4-momenta pairs. Therefore, we can rewrite $\Phi(p, q_1, q_2, q_3)$ as

$$\Phi(p, q_1, q_2, q_3) = \frac{m_Z^4}{4} \sum_{k=1,2,3} E_k^2 (m_Z - 2E_k)^2. \tag{21}$$

Notice that this expression is symmetric under the change of final photons, a reasonable behavior since there is no preferred photon in this decay. As the phase space integral also enjoys this symmetry, we can simply use one

of the terms above to do the integration and multiply the output by three, since they will necessarily give the same result. The partial width is defined as

$$d\Gamma = \frac{1}{3!} \frac{1}{2m_Z} \langle |\mathcal{M}|^2 \rangle d\Pi_3, \tag{22}$$

where $1/3!$ is the the symmetry factor due to the identical photons in the final state. The three-body phase-space function is

$$\begin{aligned}
d\Pi_3 = & \frac{d^3\mathbf{q}_1}{(2\pi)^3 2E_1} \frac{d^3\mathbf{q}_2}{(2\pi)^3 2E_2} \frac{d^3\mathbf{q}_3}{(2\pi)^3 2E_3} \\
& \times (2\pi)^4 \delta^4(p - q_1 - q_2 - q_3). \tag{23}
\end{aligned}$$

We have then

$$\begin{aligned}
d\Gamma = & K \frac{E_3(m_Z - 2E_3)^2}{E_1 E_2} d^3\mathbf{q}_1 d^3\mathbf{q}_2 d^3\mathbf{q}_3 \\
& \times \delta^4(p - q_1 - q_2 - q_3), \tag{24}
\end{aligned}$$

where the constant K, already including the factor of three, is

$$K = \frac{s_\theta^2 c_\theta^6 m_Z^3}{1536\pi^5 \beta^4}. \tag{25}$$

The rest of the calculation follows a path similar to the textbook calculation of muon decay [40]. The delta function may be split into two factors enforcing energy and 3-momentum conservation. The latter allows us to write $\mathbf{q}_2 \rightarrow -(\mathbf{q}_1 + \mathbf{q}_3)$ and $E_2 \rightarrow |\mathbf{q}_1 + \mathbf{q}_3|$. Let us take the polar axis along \mathbf{q}_3 , which is held fixed, so that

$$\begin{aligned}
E_2(\cos\theta) = & |\mathbf{q}_1 + \mathbf{q}_3| \\
= & \sqrt{E_1^2 + E_3^2 + 2E_1 E_3 \cos\theta}. \tag{26}
\end{aligned}$$

We may then write $d^3\mathbf{q}_1 = 2\pi E_1^2 d|\mathbf{q}_1| d\cos\theta$ and we have

$$\begin{aligned}
d\Gamma = & 2\pi K \frac{E_1 E_3 (m_Z - 2E_3)^2}{|\mathbf{q}_1 + \mathbf{q}_3|} d^3\mathbf{q}_3 dE_1 d\cos\theta \\
& \times \delta[g(\cos\theta)], \tag{27}
\end{aligned}$$

where $g(\cos\theta) = m_Z - E_1 - E_2(\cos\theta) - E_3$.

Now, the delta function cannot be directly integrated, so we need to change variables. This redefinition leads to

$$\delta[g(\cos\theta)] = \frac{E_2(\cos\theta)}{E_1 E_3} \delta(\cos\theta - \cos\theta_0), \tag{28}$$

where $\cos\theta_0$ is such that $g(\cos\theta_0) = 0$. The delta function now implies that both the maximum energy of any individual photon and the minimum energy of any pair of photons are $m_Z/2$. Consequently, we have E_1 and E_3 limited to the ranges $(\frac{m_Z}{2} - E_3, \frac{m_Z}{2})$ and $(0, \frac{m_Z}{2})$, respectively. Performing the remaining integrations and dividing by the Z-boson width we find that the branching ratio is given by

$$\begin{aligned}
\text{BR}(Z \rightarrow 3\gamma)_Y = & \frac{s_\theta^2 c_\theta^6}{184320\pi^3 \Gamma_{\text{exp}}^Z} \frac{m_Z^9}{\beta^4} \\
= & 6.7 \times 10^{-7} \left(\frac{m_Z}{\sqrt{\beta}} \right)^8. \tag{29}
\end{aligned}$$

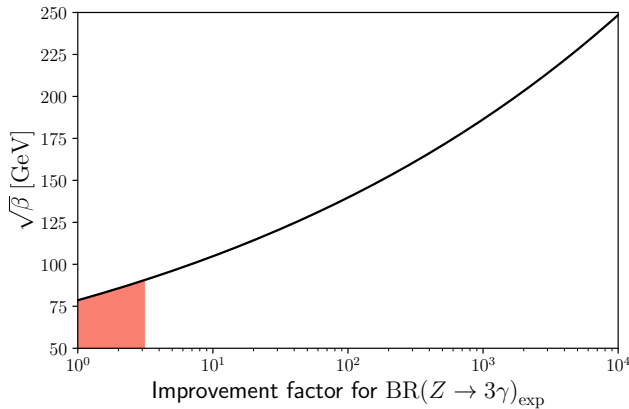


Figure 2. Projection for the lower bound on $\sqrt{\beta}$ as a function of the improvement factor of the experimental sensitivity relative to the currently best one, cf. eq. (14) [36]. Incidentally, eq. (29) reaches the order of magnitude of the SM prediction with $\sqrt{\beta} \sim 220$ GeV. The region shaded in red is such that $\sqrt{\beta} < m_Z$, where our predictions are not accurate.

We are finally able to place an experimental bound on β . The branching ratio predicted by the SM is extremely small ($\sim 10^{-10}$), way below current experimental sensitivities. Allowing the result above to fully saturate the experimental upper limit, *i.e.*, $\text{BR}(Z \rightarrow 3\gamma)_Y \simeq \text{BR}(Z \rightarrow 3\gamma)_{\text{exp}}$, cf. eq. (14). This implies that

$$\sqrt{\beta} \gtrsim 80 \text{ GeV}, \quad (30)$$

which is slightly lower than the currently best bound [26]. In ref. [41] the authors adopt the result of eq. (30) above on the BI parameter to make estimates on the redshift and to discuss birefringence and dichroism in connection with a class of p-extended BI-type actions in the presence of an external uniform magnetic field.

Here we must add an important remark. The energy scale of a decay process is set by the mass of the decaying particle, here given by $m_Z = 91.2$ GeV. Therefore, the bound obtained above must be taken with a grain of salt since it represents a mass scale lower than the energy of the process, challenging the basic assumption behind our effective-theory approach. Nonetheless, it is worth noticing that this restriction is a matter of experimental limitation: the best bound on the Z-decay into three photons is still orders of magnitude away from the SM prediction, so we may confidently expect that future experiments will yield much more stringent bounds on it, therefore significantly improving on the result above.

The lower bound in eq. (30) is clearly limited by the experimental sensitivity. If the current experimental upper bound on the branching ratio (cf. eq. (14)) would be improved by a factor of ~ 3 – a smaller improvement than the one from ATLAS [36] relative to LEP [37] – we would be able to exclude the region $\sqrt{\beta} \lesssim m_Z$. Future lepton colliders, *e.g.*, ILC [42–45] and FCC-ee [46, 47], whose

main goal is precision Higgs physics, could operate at the Z-pole and produce a vast sample of Z-bosons: the ILC and the FCC-ee could produce respectively 10^2 and 10^5 times more Z-bosons than LEP. It is therefore possible, with much better statistics and improved detector capabilities, to improve the upper limit on $\text{BR}(Z \rightarrow 3\gamma)$ enough to constrain $\sqrt{\beta}$ at or above m_Z .

In fig. 2 we plot the lower bound on $\sqrt{\beta}$ as a function of the future improvement of the experimental sensitivity, $\text{BR}(Z \rightarrow 3\gamma)_{\text{exp}}$, relative to the currently best one [36]. The situation discussed in the paragraph above is illustrated by the area shaded in red: an improvement of at least ~ 3 would lead to viable bounds. The unfortunately weak dependence of the expansion parameter on the experimental sensitivity is made explicit by the slope of the curve, meaning that only large improvements in sensitivity would lead to noticeable improvements in the lower bound on our non-linear extension.

As a final remark we note that the discussion above relies on the fact that, so far (and in the foreseeable future), only upper limits on the process $Z \rightarrow 3\gamma$ could be placed. The SM prediction is four orders of magnitude below the currently best upper bound, so we may also speculate about possible limits on the expansion parameter in case the SM expectation is eventually confirmed. In this scenario there is no tension between the SM and experiment, so we may assume that the non-standard result is responsible for a small correction of the SM prediction, being hidden under the (relative) experimental uncertainty, *i.e.*, $\text{BR}_Y(\beta)/\text{BR}_{\text{SM}} \lesssim \delta_{\text{exp}}$. Conservatively assuming $\delta_{\text{exp}} \sim 10\%$ would allow us to place the strong lower bound $\sqrt{\beta} \gtrsim 295$ GeV.

B. $e^- e^+ \rightarrow 3\gamma$

Hadron colliders have played a central role in the establishment of the SM as our best theory of elementary particles and their interactions; great examples are the discoveries of the W- and Z-bosons, as well as of the Higgs scalar. However, lepton colliders, such as LEP, were crucial in subsequent precision measurements, helping to probe not only tree-level predictions, but also radiative corrections [48]. The next development is to achieve even higher precision in measurements of electroweak parameters, in particular those related to the Higgs and gauge bosons [49].

Lepton colliders represent optimal tools to this end and next-generation machines have been proposed, such as ILC [42–45], FCC-ee [46, 47], CEPC [50] and CLIC [51]. These are designed to study the SM in great detail, but searching for deviations from the SM that could hint at new physics is an equally important goal. In this context, the process $e^- e^+ \rightarrow 3\gamma$ offers an interesting option to test modifications of the gauge couplings, in particular those involving photons and Z-bosons. From eq. (13) we see that our non-linear extension induces precisely such

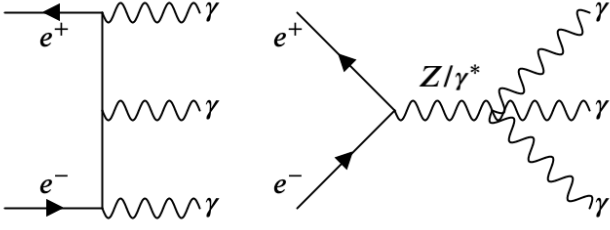


Figure 3. The lowest-order Feynman diagrams contributing to the scattering $e^-(p_1) e^+(p_2) \rightarrow \gamma(q_1) \gamma(q_2) \gamma(q_3)$.

anomalous couplings that could give rise to new contributions for processes with three photons in the final state. We note that the SM contribution is very well described by QED with negligible electroweak corrections.

The Feynman diagrams contributing to $e^- e^+ \rightarrow 3\gamma$ at tree level are shown in fig. 3. The QED contribution is given by

$$-i\mathcal{M}_{\text{QED}} = ie^3 \bar{v}(p_2) \left[\gamma^\rho \frac{\not{p}_1 - \not{q}_1 - \not{q}_2}{(p_1 - q_1 - q_2)^2} \gamma^\nu \right. \\ \left. \times \frac{\not{p}_1 - \not{q}_1}{(p_1 - q_1)^2} \gamma^\mu \right] u(p_1) \epsilon_\mu^*(q_1) \epsilon_\nu^*(q_2) \epsilon_\rho^*(q_3), \quad (31)$$

which must be added to the other five amplitudes obtained from this one by permutation of the external photons. We are considering high-energy scatterings, so the electron mass may be safely neglected. The non-linearly induced photon- and Z-mediated amplitudes are given by

$$-i\mathcal{M}_\gamma = \frac{-e}{(p_1 + p_2)^2} \bar{v}(p_2) \gamma_\mu u(p_1) \\ \times V_{4\gamma}^{\mu\nu\beta\rho}(\beta) \epsilon_\nu^*(q_1) \epsilon_\beta^*(q_2) \epsilon_\rho^*(q_3), \quad (32)$$

$$-i\mathcal{M}_Z = \frac{g_Z}{(p_1 + p_2)^2 - m_Z^2 + im_Z \Gamma_Z} \\ \times \bar{v}(p_2) \gamma_\mu (c_v - c_a \gamma^5) u(p_1) \\ \times V_{Z3\gamma}^{\mu\nu\beta\rho}(\beta) \epsilon_\nu^*(q_1) \epsilon_\beta^*(q_2) \epsilon_\rho^*(q_3), \quad (33)$$

where $g_Z = e/4s_\theta c_\theta$, $c_v = -1 + 4s_\theta^2$ and $c_a = -1$. The Z-width is $\Gamma_Z = 2.49$ GeV. The $Z\gamma\gamma\gamma$ vertex was defined in eq. (16) and the four-photon vertex is analogous:

$$V_{4\gamma}^{\alpha\beta\gamma\delta}(\beta) = i \frac{c_\theta^4}{\beta^2} f^{\alpha\beta\gamma\delta}. \quad (34)$$

The function $f^{\alpha\beta\gamma\delta}$ is given by eq. (17) with the appropriate relabelling of the 4-momenta.

The total tree-level amplitude for the process, \mathcal{M} , is $\mathcal{M} = \mathcal{M}_{\text{QED}} + \mathcal{M}_\gamma + \mathcal{M}_Z$ and the total unpolarized cross section is given by

$$d\sigma = \frac{1}{3!} \frac{1}{2E_{\text{cm}}^2} \langle |\mathcal{M}|^2 \rangle d\Pi_3, \quad (35)$$

where $1/3!$ is the symmetry factor due to the identical photons in the final state and the phase-space factor is the same as in eq. (23). The squared amplitude is essentially the sum of three contributions: a pure QED part, an interference term between QED and the non-linear amplitudes, and a purely non-linear term. The contribution from pure QED is discussed in app. A.

Let us first discuss the interference term, $\langle |\mathcal{M}|_{\text{QED-Y}}^2 \rangle$. The unpolarized squared amplitude is quoted in detail in app. B. To simplify matters, we may express all energies and 3-momenta in units of the CM energy, E_{cm} , so that we can write it as

$$\langle |\mathcal{M}|_{\text{QED-Y}}^2 \rangle = \mathcal{X}_{\text{QED-Y}} e^4 c_\theta^2 \frac{E_{\text{cm}}^2}{\beta^2} \mathcal{A}(p_i, q_j), \quad (36)$$

with $\mathcal{A}(p_i, q_j)$ representing a function of the now dimensionless energies and 3-momenta that the reader may obtain from eq. (B1). The pre-factor $\mathcal{X}_{\text{QED-Y}}$ is given by ($x = m_Z^2/E_{\text{cm}}^2$ and $y = \Gamma_Z^2/m_Z^2$)

$$\mathcal{X}_{\text{QED-Y}} = \frac{3 - (3 + 4c_\theta^2)x + 4c_\theta^2 x^2(1 + y)}{(1 - x)^2 + yx^2}. \quad (37)$$

From the phase-space volume we get another factor of E_{cm}^2 that cancels the one present in the denominator of eq. (35), so that, putting all the numerical factors together, we finally obtain

$$\sigma(e^- e^+ \rightarrow 3\gamma)_{\text{QED-Y}} = \mathcal{X}_{\text{QED-Y}} \frac{\alpha^2 c_\theta^2}{384\pi^3} \frac{s}{\beta^2} \mathcal{I}_{\text{QED-Y}} \quad (38)$$

with $s = E_{\text{cm}}^2$, $e^2 = 4\pi\alpha$ and

$$\mathcal{I}_{\text{QED-Y}} = \int \mathcal{A}(p_i, q_j) \frac{d^3\mathbf{q}_1}{E_1} \frac{d^3\mathbf{q}_2}{E_2} \frac{d^3\mathbf{q}_3}{E_3} \delta^4(\Sigma p_i - \Sigma q_j). \quad (39)$$

Note that the quantities in eq. (39) are all expressed in units of $\sqrt{s} = E_{\text{cm}}$, being therefore dimensionless.

Equation (39) cannot be easily evaluated analytically due to the complexity of the integrand, so we solve it numerically via standard Monte Carlo methods. The Dirac delta enforcing 4-momentum conservation severely constrains the phase-space volume available to the outgoing photons. In fact, their individual energies are bound to be at most 0.5 and the sum of any pair of energies must be larger than this value, allowing us to limit the range of the sampled 3-momentum components to the interval $[-0.5, 0.5]$. In what follows we use data from $e^- e^+$ collisions at LEP resulting in two or three photons and the cross sections quoted were obtained under the experimental conditions of the detector. That means that we have to impose similar cuts to our theoretical cross sections if we want to compare them to LEP data.

Particularly important are the angular and energy cuts imposed [52, 53]. Since the forward-backward direction along the beam is inaccessible, the range in polar angles is limited to $16^\circ \leq \theta_\gamma \leq 164^\circ$, *i.e.*, the detectable photons must satisfy $|\cos\theta_\gamma| \leq 0.96$ to be contained in the

electromagnetic calorimeter. Furthermore, the individual photons must have an energy $E_\gamma > 5$ GeV. Even though eq. (39) is written in terms of dimensionless quantities, the aforementioned lower threshold on the detectable energy of the single photons introduces an energy dependence, as the cut is expressed as $E_\gamma > 5/\sqrt{s}$. The values of the integral evaluated at selected energy values are quoted in table I. For the sake of concreteness, the interference cross section at $\sqrt{s} = 207$ GeV is

$$\sigma_{\text{QED-Y}}(\sqrt{s} = 207 \text{ GeV}) \simeq 0.88 \left(\frac{250 \text{ GeV}}{\sqrt{\beta}} \right)^4 \text{ fb}. \quad (40)$$

We now move on to the the purely non-linear contribution, $\langle |\mathcal{M}|_Y^2 \rangle$, which is expected to be sub-dominant relative to the interference term discussed above. The unpolarized squared amplitude is stated in eq. (B5) and, after expressing the 4-momenta in units of E_{cm} , we have

$$\langle |\mathcal{M}|_Y^2 \rangle = \mathcal{X}_Y e^2 c_\theta^4 \frac{E_{\text{cm}}^6}{\beta^4} \mathcal{B}(p_i, q_j), \quad (41)$$

with $\mathcal{B}(p_i, q_j)$ represents a dimensionless function in analogy with $\mathcal{A}(p_i, q_j)$. The pre-factor is

$$\mathcal{X}_Y = \frac{5 - 12c_\theta^2 x + 8c_\theta^4 x^2(1+y)}{(1-x)^2 + yx^2}. \quad (42)$$

Equation (41) may be integrated analytically¹, but here we adopted the same Monte Carlo set-up employed in the calculation of the interference term. The cross section is then given by

$$\sigma(e^-e^+ \rightarrow 3\gamma)_Y = \mathcal{X}_Y \frac{\alpha c_\theta^4}{6144\pi^4} \frac{s^3}{\beta^4} \mathcal{I}_Y, \quad (43)$$

where \mathcal{I}_Y is defined analogously to $\mathcal{I}_{\text{QED-Y}}$, cf. eq. (39). Specializing to $\sqrt{s} = 207$ GeV and using the numerical value of the integral including detector cuts from table I, we have

$$\sigma_Y(\sqrt{s} = 207 \text{ GeV}) \simeq 0.01 \left(\frac{250 \text{ GeV}}{\sqrt{\beta}} \right)^8 \text{ fb}. \quad (44)$$

In the discussion above we have obtained the total cross sections involving the novel neutral vertices originating in eq. (13). The fact that only quartic vertices are produced implies that $e^-e^+ \rightarrow 2\gamma$ does not receive corrections, at least at tree level, but $e^-e^+ \rightarrow 3\gamma$ does. From dimensional analysis alone we expect the number of events with two photons to be roughly two orders of magnitude times larger than with three photons, thus making dedicated searches for three-photon events harder. Therefore, more commonly, experiments look for multi-photon processes and the best available data to our

\sqrt{s} [GeV]	91.2	207	250	350
\mathcal{I}_{QED}	27006	37976	41796	45854
$\mathcal{I}_{\text{QED-Y}}$	19.45	20.02	20.13	20.24
\mathcal{I}_Y	0.138	0.139	0.139	0.139

Table I. Values of the numerical integrals appearing in eqs. (38), (43) and (A7). The first two energy values are relevant in the context of existing LEP data [52, 53], whereas the last two are important for future e^-e^+ colliders, such as the ILC [42–45, 55]. The following cuts were applied: $E_\gamma > 5$ GeV and $|\cos\theta_\gamma| < 0.96$ [52, 53].

knowledge were collected at LEP where the CM energy of the e^-e^+ pair was scanned passing by the Z-pole and reaching more than 200 GeV.

The L3 collaboration analyzed LEP data of events resulting in multiphoton final states [52, 53]. Since electroweak corrections are heavily suppressed, these measurements provide a clean test of QED, whose predictions were successfully confirmed. The calculations of the QED expectation were performed following ref. [54], where contributions up to $\mathcal{O}(\alpha^3)$ are considered, *i.e.*, the tree-level cross sections for two and three final photons plus radiative corrections. Here, however, we are working with an effective theory and we limit our analysis to tree level and we refrain from employing their results.

The tree-level cross section for $e^-e^+ \rightarrow 2\gamma$ is well known, cf. eq. (A2). No closed form for the tree-level cross section for $e^-e^+ \rightarrow 3\gamma$ in the CM could be found, so we calculated the squared amplitude analytically and performed the phase-space integration numerically including the appropriate detector cuts; cf. eq (A8). Let us consider concrete data to try to constrain $\sqrt{\beta}$. Since we are dealing with an effective theory whose effects grow with energy, we will ignore data at the Z-pole [52] and focus on the more promising high-energy results [53].

The L3 collaboration analyzed $e^-e^+ \rightarrow \gamma\gamma(\gamma)$ data in detail and indicates cross-section measurements for final states with two and three photons. The highest energy bin is 207 GeV (cf. table 3 of ref. [53]) and they quote the expected $\mathcal{O}(\alpha^3)$ cross section as 9.9 pb, whereas our tree-level result is 9.2 pb. Given that the difference includes radiative contributions deliberately unaccounted for here and possible effects from further selection criteria, we are confident that our calculation delivers a meaningful result for the QED prediction at tree-level.

Now, given that QED accurately describes the experimental data, we are only able to find lower bounds on $\sqrt{\beta}$. In fact, we may constrain it by demanding that the effects of the non-linear extension hide under the relative experimental uncertainty

$$\frac{\sigma_{\text{QED-Y}} + \sigma_Y}{\sigma_{\text{QED}}} \lesssim \delta_{\text{exp}}, \quad (45)$$

with σ_{QED} being the tree-level expectation from QED.

¹ The result without detector cuts is: $\sigma_Y = \mathcal{X}_Y \frac{\alpha c_\theta^4}{368640\pi^2} \frac{s^3}{\beta^4}$.

The cross sections for final states with two and three photons are respectively $\sigma_{\text{QED}}^{2\gamma}$, eq. (A2), and $\sigma_{\text{QED}}^{3\gamma}$, eq. (A8). For the sake of concreteness, we focus on the highest energy bin quoted in table 3 from ref. [53], $\sqrt{s} = 207$ GeV, for which the relative uncertainty of the measured cross section is $\delta_{\text{exp}} = 0.34/10.16 \simeq 0.034$. Plugging this and $\sigma_{\text{QED}}^{2\gamma} + \sigma_{\text{QED}}^{3\gamma} = 9.2$ pb into eq. (45), we obtain $\sqrt{\beta} \gtrsim 73$ GeV.

The absolute number of $e^-e^+ \rightarrow 3\gamma$ events is also reported in ref. [53] for different energies, albeit without the respective experimental uncertainties. Focusing again on $\sqrt{s} = 207$ GeV, the expected tree-level cross section for pure QED is 0.29 pb. At this energy, 29 three-photon events were observed, so we may conservatively assume that the uncertainty is $\sim \sqrt{29} \simeq 5.4$ events. Taking into account the effective integrated luminosity, 87.8 pb^{-1} , this is equivalent to 0.06 pb, so that the relative uncertainty is $\delta_{\text{exp}} = 0.06/0.29 \simeq 0.21$. With $\sigma_{\text{QED}} = \sigma_{\text{QED}}^{3\gamma} = 0.29$ pb, eq. (45) gives $\sqrt{\beta} \gtrsim 97$ GeV.

The bounds found above suffer from the same limitation as the one from the analysis of Z-decay: $\sqrt{\beta} < \sqrt{s}$. This is, however, not surprising, since the experimental uncertainties are orders of magnitude larger than the typical values expected from eqs. (40) and (44). We are thus confronted with the fact that the currently available data on $e^-e^+ \rightarrow \gamma\gamma(\gamma)$ do not yield viable bounds on $\sqrt{\beta}$.

Despite being experimentally more challenging, measuring $e^-e^+ \rightarrow 3\gamma$ has the largest potential, as only the process directly affected by the non-linear effects is examined. We conclude, therefore, that a sensible lower limit on $\sqrt{\beta}$ could be placed if future e^-e^+ colliders would include measuring this process in their research programs. Let us take the ILC as an example, which targets a total integrated luminosity of 14 ab^{-1} over its full operation time [55]. For the sake of clarity, let us focus on the initial stage with $\sqrt{s} = 250$ GeV, where an integrated luminosity of $\sim 500 \text{ fb}^{-1}$ is planned to be attained in the first five years. Assuming similar detector cuts as at LEP and a (pessimistic) 1% effective luminosity², $\sim 5 \text{ fb}^{-1}$, pure QED predicts 1073 three-photon events, whereas the non-linear terms would contribute with extra 3 events for $\sqrt{\beta} = 300$ GeV, *i.e.*, the level of precision required would be $3/1073 \sim 0.3\%$. A similar precision would be required at $\sqrt{s} = 350$ GeV with $\sqrt{\beta} = 400$ GeV.

C. Pure gauge-boson scatterings

The SM is based on the non-Abelian gauge group $SU(2)_L \times U(1)_Y$. This is manifest in the form of the covariant derivative, cf. eq. (4), and the non-linear transformation properties of the gauge bosons. Particularly

² For comparison, the analysis of $e^-e^+ \rightarrow \gamma\gamma(\gamma)$ at LEP in the energy range 192 – 209 GeV contained 0.43 fb^{-1} of data, roughly ten times less.

relevant is the presence of not only quadratic, but also triple and quartic self-interaction couplings. As a matter of fact, in a pure Yang-Mills theory, the quartic coupling is related to the triple one, even at the quantum level, as a consequence of gauge symmetry – this is a trade-mark feature of a non-Abelian theory. As the SM is tested with increasing accuracy, the structure of the theory may also be probed and possible deviations identified.

Of special interest from both theoretical and experimental points of view are measurements of the gauge self-couplings, in particular those involving the Z-boson and the photon. With this in mind, we consider some of the possible scattering processes proceeding via the quartic couplings from eq. (13) already at tree level.

1. $\gamma\gamma \rightarrow ZZ$

As mentioned in sec. IIIB, e^-e^+ colliders offer clean conditions for precision tests of the SM. More interestingly, there are currently proposals of machines that can be adapted to work as linear photon colliders, such as TESLA [56] or the ILC [42, 57], which would use the Compton back scattering of electrons in lasers to produce $\gamma\gamma$ or $e\gamma$ collisions [58]. In this scenario, the photons would carry $\sim 80\%$ of the initial CM energy, *i.e.*, $\sqrt{s_{\gamma\gamma}} \approx 0.8\sqrt{s_{ee}}$ [59], thus amounting to CM energies of up to $\sqrt{s_{\gamma\gamma}} \approx 400$ GeV and $\sqrt{s_{\gamma\gamma}} \approx 800$ GeV for the TESLA and ILC designs, respectively.

Since we are studying a modification to the gauge sector of the SM, let us focus on $\gamma\gamma$ collisions producing exclusively vector bosons $V_i = \gamma, Z, W^\pm$. In this context, following ref. [56] (in particular fig. 1.1.2), measuring the process $\gamma\gamma \rightarrow W^+W^-$ in a photon collider is one of the highest priorities, as its total cross section is roughly constant at 80 pb [60–62], which is followed by $\gamma\gamma \rightarrow W^+W^-Z$ reaching ~ 5 fb at 300 GeV. Both would receive no tree-level corrections due to the non-linear terms in eq. (13). Incidentally, $\gamma\gamma \rightarrow \gamma\gamma$, which has a QED cross section of $\sim 10^{-30}$ pb [63, 64], has already been considered in ref. [26], so we ignore it here.

The next most relevant contribution is $\gamma\gamma \rightarrow ZZ$. Within the framework of the SM, this process cannot take place at tree level, but it will in fact receive a tree-level contribution from our non-linear extension. Similarly to $\gamma\gamma \rightarrow W^+W^-$, Z-pair production may be used to study the gauge structure of the SM and Higgs physics [65, 66]. It is therefore an important process in future photon colliders and in the following we calculate the non-linear contribution to the cross section at tree level.

From eq. (13) we see that the vertex factor is simply

$$V_{\gamma\gamma ZZ}^{\alpha\beta\gamma\delta}(\beta) = i \frac{s_\theta^2 c_\theta^2}{\beta^2} f^{\alpha\beta\gamma\delta}, \quad (46)$$

with $f^{\alpha\beta\gamma\delta}$ again given by eq. (17), but with the substitutions: $p \rightarrow p_1, q_1 \rightarrow -p_2, q_2 \rightarrow q_1$ and $q_3 \rightarrow q_2$, since here

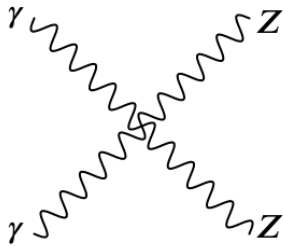


Figure 4. The lowest-order Feynman diagram contributing to the scattering $\gamma(p_1)\gamma(p_2) \rightarrow Z(q_1)Z(q_2)$.

we are dealing with a 2-to-2 scattering and not a decay. The tree-level amplitude for this process then becomes

$$-i\mathcal{M} = \epsilon_\alpha(p_1)\epsilon_\beta(p_2)V_{\gamma\gamma ZZ}^{\alpha\beta\gamma\delta}(\beta)\epsilon_\gamma^*(q_1)\epsilon_\delta^*(q_2) \quad (47)$$

with the momenta attributions given in fig. 4. Here we are assuming that the unpolarized photons are on shell and monochromatic. This is a simplified scenario and a more detailed analysis would follow the strategy from ref. [26].

After summing and averaging over polarizations, the unpolarized squared amplitude is found to be

$$\begin{aligned} \langle |\mathcal{M}|^2 \rangle &= \frac{s_\theta^4 c_\theta^4}{8\beta^4} [m_Z^4 s^2 + s^2 (s - 2m_Z^2)^2 \\ &\quad + (t - m_Z^2)^4 + (u - m_Z^2)^4], \end{aligned} \quad (48)$$

where the Mandelstam variables, expressed in terms of the CM energy E_{cm} of the incoming photons and the scattering angle θ , are

$$s = E_{\text{cm}}^2, \quad (49a)$$

$$t = m_Z^2 - \frac{s}{2}(1 - \beta_Z \cos \theta), \quad (49b)$$

$$u = m_Z^2 - \frac{s}{2}(1 + \beta_Z \cos \theta). \quad (49c)$$

Here $\beta_Z = \sqrt{1 - 4m_Z^2/s}$ is the velocity of either of the outgoing Z-bosons, not to be confused with the non-linear expansion parameter, β .

Finally, setting $x = m_Z^2/s$, the total cross section is

$$\begin{aligned} \sigma(\gamma\gamma \rightarrow ZZ)_Y &= \frac{s_\theta^4 c_\theta^4}{1280\pi} \frac{s^3}{\beta^4} \sqrt{1 - 4x} \\ &\quad \times (7 - 26x + 27x^2). \end{aligned} \quad (50)$$

This result is shown in black in fig. 5 for $\sqrt{\beta} = 250$ GeV. If the non-linear hypercharge sector is indeed realized in Nature, the expression above would provide the only tree-level contribution to the cross section, since this process cannot take place in the SM at this order. In fact, the first SM contribution is generated via fermion and W-boson loops [65, 66] with a cross section of ~ 20 fb shortly above threshold and roughly saturating at ~ 200 fb for CM energies $\gtrsim 800$ GeV [56].

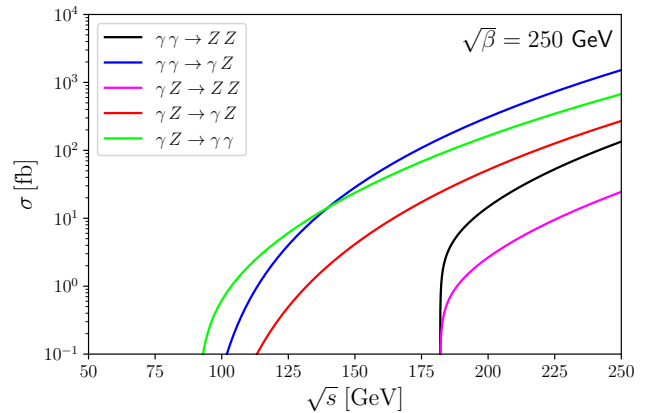


Figure 5. Total cross sections for selected processes involving only the quartic vertices from eq. (17) in the CM. Here we set $\sqrt{\beta} = 250$ GeV, but the scaling for other values can be easily performed via eq. (51).

Process	N	$\kappa(x)$	$F(x)$
$\gamma\gamma \rightarrow ZZ$	$\frac{s_\theta^4 c_\theta^4}{1280\pi}$	$\sqrt{1 - 4x}$	$7 - 26x + 27x^2$
$\gamma\gamma \rightarrow \gamma Z$	$\frac{s_\theta^2 c_\theta^6}{1920\pi}$	$(1 - x)^3$	$21 + 3x + x^2$
$\gamma Z \rightarrow ZZ$	$\frac{s_\theta^6 c_\theta^2}{5760\pi}$	$(1 - x)\sqrt{1 - 4x}$	$21 - 75x + 98x^2 - 20x^3 + 6x^4$
$\gamma Z \rightarrow \gamma Z$	$\frac{s_\theta^4 c_\theta^4}{2880\pi}$	$(1 - x)^4$	$21 + 6x + 16x^2 + 6x^3 + 6x^4$
$\gamma Z \rightarrow \gamma\gamma$	$\frac{s_\theta^2 c_\theta^6}{5760\pi}$	$(1 - x)$	$21 + 3x + x^2$

Table II. Total cross sections for processes involving only quartic couplings of neutral gauge bosons, cf. eq. (51) with $x = m_Z^2/s$. These results are shown in fig. 5 for $\sqrt{\beta} = 250$ GeV.

2. Other pure quartic gauge couplings

The general structure of the calculation is similar to that of the previous section on $\gamma\gamma \rightarrow ZZ$, since the vertex factor is the same as in eq. (46) and the only diagram contributing to the process at tree level is analogous to the one shown in fig. 4. Clearly, the amplitude will be similar to eq. (48), some of them are related by crossing symmetry, so we do not write it explicitly here.

The total cross section for these processes can be written in a systematic way by factoring numerical factors N , kinematic and phase-space factors $\kappa(x)$ and further energy-dependent contributions $F(x)$, that is,

$$\sigma = N \left(\frac{s^3}{\beta^4} \right) \kappa(x) F(x) \quad (51)$$

with $x = m_Z^2/s$.

IV. CONCLUDING REMARKS

Motivated by recent results in the physics of electroweak monopoles, we investigated the consequences of a non-linear extension in the weak hypercharge sector in high-energy processes. The proposed extension is characterized by a parameter $\sqrt{\beta}$ with dimension of mass, which may be used to perform a Taylor expansion in $X = \frac{\mathcal{F}}{\beta^2} - \frac{\mathcal{G}^2}{2\beta^4}$, cf. eq. (12). After EW symmetry breaking we obtain a series of quartic, dimension-eight effective operators involving the photon and Z-boson that are absent from the SM at tree level, cf. eq. (13).

In this context, we have analyzed a few interesting processes, namely, Z-decay and electron-positron annihilation, both resulting in three photons as final products, and Z-boson production via photon fusion. The first and most promising one, Z-decay, is a rare process occurring only at loop level in the SM, but induced at tree level by non-linear effects. The expected impact of the non-linear vertex on the branching ratio is a factor ~ 3 too small, cf. eq. (29). This is due to the still loose experimental upper bound on the branching ratio of Z-decay into three photons, which is four orders of magnitude larger than the value predicted by the SM.

Future e^-e^+ colliders, such as the ILC or FCC-ee, may operate at the Z-resonance and produce a large amount of Z-bosons – up to a factor 10^5 more than at LEP – thereby dramatically increasing the statistics for measuring the products of Z-decay. We are therefore confident that the experimental upper limit on the branching ratio will be significantly improved in the near future, thus enabling us to set more stringent bounds on $\sqrt{\beta}$, readily excluding the range $\sqrt{\beta} \lesssim m_Z$, cf. fig. 2. We remark that, in a scenario where experiment reaches the level of the SM prediction, lower bounds ~ 200 GeV could be set.

The second process analyzed was electron-positron annihilation into three photons, also a relatively rare process. It is well described by QED and the non-linear extension provides small corrections also at tree level, cf. fig. 3. We have calculated the unpolarized cross sections of pure QED, pure non-linear and interference effects at the CM. Since there is no tension between the predictions from QED and the experimental data, we have used the (relative) experimental uncertainties from LEP data for $e^-e^+ \rightarrow \gamma\gamma(\gamma)$ and $e^-e^+ \rightarrow 3\gamma$ above the Z-pole to derive lower bounds on $\sqrt{\beta}$.

The process with two- and three-photon final states is well measured, but the non-linear effects, which contribute only to $e^-e^+ \rightarrow 3\gamma$, are shadowed by the much larger QED contribution, $e^-e^+ \rightarrow 2\gamma$. The data on exclusively three-photon final states is not so complete, but a conservative estimate delivers a somewhat better lower bound on $\sqrt{\beta}$. The non-linear effects are much smaller than the available precision and it was not possible to obtain viable bounds with the current experimental data, but we project that the necessary improvements may be within the reach of the next-generation lepton colliders.

Finally, we have also analyzed selected scattering processes involving exclusively neutral gauge bosons. The unpolarized tree-level cross sections may reach a few hundred fb at $\sqrt{s} = 200$ GeV for $\sqrt{\beta} = 250$ GeV, cf. fig. 5. These processes are good candidates to detect possible signatures from the non-linear extension in future experiments, given that they occur only at loop level in the SM, but are induced at tree level, cf. eq. (13).

Quite generally, we expect the non-linear effects to be heavily suppressed by $\sqrt{\beta}$ – it could reach TeV energies depending on the underlying beyond the SM scenario. In this work we have tried to constrain $\sqrt{\beta}$ with high-energy experiments and we saw that, in order to have any chance to detect such effects, very precise measurements are needed. A good example is the Z-decay into three photons for which the (minute) SM contribution is generated at loop level, whereas the non-linear effects contribute already at tree level. This, together with the optimistic prospect of an improved upper limit on the branching ratio, makes this process a very promising way to search for the effects outlined in this work.

This can be contrasted to the situation with electron-positron annihilation: the non-linear effects are orders of magnitude smaller than the SM results and thus very hard to detect – like finding a needle in a haystack. We can see this by comparing the magnitudes of the cross sections in eqs. (40) and (44), ~ 0.9 fb for $\sqrt{\beta} = 250$ GeV, with the size of the experimental uncertainties quoted in ref. [53], ~ 0.5 pb. Since the non-linear contributions are much smaller than the uncertainties involved, the only way to make them comparable (*à la* eq. (45)) is by having $\sqrt{\beta} \lesssim \sqrt{s}$ to effectively enhance the non-linear effects.

To conclude our contribution, we remark that a more general implementation of the non-linear extension of the electroweak sector is possible. Here we have considered the $U(1)_Y$ sector, but an analogous modification may be performed in the $SU(2)_L$ sector. In this case, the already analyzed neutral sector would receive small modifications, but interesting non-linear effects would be also induced in the charged sector of the SM. This will be the subject of another work to appear soon.

ACKNOWLEDGMENTS

PDF thanks specially G.P. de Brito for interesting discussions and technical support, is grateful to Natanael C. Costa for the discussions about Monte Carlo methods and also thanks W.B. de Lima and G. Picanço for helpful discussions. PCM is grateful to S.F. Amato and E. Polcarpo for their support with the experimental results and also thanks D. Kroff for helpful discussions. PDF thanks the Brazilian scientific support agencies, CNPq and FAPERJ, for financial support. PCM dedicates this paper to his soon to be born daughter, Marina.

Appendix A: Tree-level QED results for $e^-e^+ \rightarrow \gamma\gamma(\gamma)$

In sec. III B we discussed the tree-level effects of the non-linear extension of the $U(1)_Y$ sector in the process $e^-e^+ \rightarrow \gamma\gamma(\gamma)$. The experimental results from LEP included cross sections with final states of two and three photons subjected to detector cuts in energy and scattering angle, namely, $E_\gamma > 5$ GeV and $|\cos\theta_\gamma| < 0.96$ [52, 53], so it is important to understand the tree-level expectation from QED to $e^-e^+ \rightarrow \gamma\gamma$ and $e^-e^+ \rightarrow \gamma\gamma\gamma$ under these conditions to be able to derive limits on β .

We start with the simplest case, $e^-e^+ \rightarrow \gamma\gamma$. Since there are two identical particles in the final state and the reaction takes place at the CM, the two photons carry the same energy as the colliding electron. Assuming monochromatic beams with energies of a few hundred GeV, the outgoing photons automatically satisfy the energy cut. The tree-level differential cross section is given by the well-known result

$$\frac{d\sigma_{\text{QED}}^{2\gamma}}{d\cos\theta} = \frac{2\pi\alpha^2}{s} \left(\frac{1 + \cos^2\theta}{1 - \cos^2\theta} \right). \quad (\text{A1})$$

For two identical particles, the polar angle is confined to the range $0 \leq \cos\theta_\gamma \leq 1 - c_{\text{cut}}$ and, integrating eq. (A1) in this range, we find³

$$\sigma_{\text{QED}}^{2\gamma} = \frac{2\pi\alpha^2}{s} \left[\log\left(\frac{2 - c_{\text{cut}}}{c_{\text{cut}}}\right) + c_{\text{cut}} - 1 \right]. \quad (\text{A2})$$

For LEP at $\sqrt{s} = 207$ GeV with $c_{\text{cut}} = 0.04$ we get 9.6 pb. It is worthwhile pointing out that the divergence in the forward-backward direction leads to a significant reduction of the total cross section even for small angular cuts.

Let us now move on to the more involved case of $e^-e^+ \rightarrow \gamma\gamma\gamma$. The typical amplitude is given in eq. (31), which must be added to other five similar contributions with permutations of the photon 4-momenta. If we define $p_{ij} = p_i \cdot q_j$ and $q_{ij} = q_i \cdot q_j$, the squared and spin-averaged amplitude can be written as

$$\langle |\mathcal{M}_{3\gamma}|^2 \rangle = \mathcal{Q} \left[p_{11} \sum_{n=0}^3 (p_1 \cdot p_2)^n Q_n + \text{perm.} \right] \quad (\text{A3})$$

where ‘‘perm.’’ indicates that we must add the expression with the photon labels reshuffled. The pre-factor is

$$\mathcal{Q} = \frac{2e^6}{(p_{11})(p_{12})(p_{13})(p_{21})(p_{22})(p_{23})} \quad (\text{A4})$$

³ In order to keep track of the forward-backward enhancement in the ultra-relativistic limit it is usually imposed that $c_{\text{cut}} = 2m_e^2/s$.

and the terms in the sum are

$$Q_0 = p_{12} \left[p_{13}p_{21}p_{22} + p_{23}(p_{11}p_{22} + p_{23}(p_{22} - q_{12}) + p_{21}(p_{22} + q_{23})) \right] - p_{11}p_{22}p_{23}q_{23}, \quad (\text{A5a})$$

$$Q_1 = p_{12} \left[p_{13}p_{21} - p_{21}(p_{22} - 4p_{23}) + p_{23}(p_{23} - q_{23}) \right] + p_{22} \left[p_{11}(-p_{22} + p_{23} + q_{23}) - p_{23}q_{12} + p_{22}q_{13} + p_{21}p_{23} \right], \quad (\text{A5b})$$

$$Q_2 = -2p_{12}p_{21} - p_{22}(2p_{21} - q_{12} + q_{13} + q_{23}), \quad (\text{A5c})$$

$$Q_3 = p_{21}. \quad (\text{A5d})$$

The final averaged squared amplitude can be symbolically recast in the form

$$\langle |\mathcal{M}_{3\gamma}|^2 \rangle = \frac{e^6}{E_{\text{cm}}^2} \mathcal{C}(p_i, q_j), \quad (\text{A6})$$

where we have expressed all dimensional parameters in terms of the CM energy – in this way $\mathcal{C}(p_i, q_j)$ is effectively dimensionless. Taking into account the phase-space volume, cf. eq. (23), the integral to be solved is

$$\mathcal{I}_{\text{QED}} = \int \mathcal{C}(p_i, q_j) \frac{d^3\mathbf{q}_1}{E_1} \frac{d^3\mathbf{q}_2}{E_2} \frac{d^3\mathbf{q}_3}{E_3} \delta^4(\Sigma p_i - \Sigma q_j), \quad (\text{A7})$$

but an analytical treatment is cumbersome, so we resort to numerical methods, which also facilitate the application of the detector cuts. The results of the Monte Carlo integral are listed in table I for a few interesting values of the CM energy. The tree-level cross section for $e^-e^+ \rightarrow \gamma\gamma\gamma$ is ($e^2 = 4\pi\alpha$)

$$\begin{aligned} \sigma_{\text{QED}}^{3\gamma} &= \frac{\alpha^3}{48\pi^2 s} \mathcal{I}_{\text{QED}} \\ &\simeq 8 \times 10^{-3} \cdot \mathcal{I}_{\text{QED}} \left(\frac{200 \text{ GeV}}{\sqrt{s}} \right)^2 \text{ fb}. \end{aligned} \quad (\text{A8})$$

Using $\sqrt{s} = 207$ GeV as an example, we have 0.285 pb.

Appendix B: Interference and purely non-linear amplitudes for $e^-e^+ \rightarrow 3\gamma$

Here we briefly present the results for the tree-level amplitudes discussed in sec. III B. The interference amplitude between pure QED and the non-linear contributions may be written as

$$\langle |\mathcal{M}_{\text{QED-Y}}|^2 \rangle = \mathcal{H} \left[\sum_{n=0}^3 (p_1 \cdot p_2)^n H_n + \text{perm.} \right] \quad (\text{B1})$$

with

$$\mathcal{H} = \frac{c_\theta^2 e^4}{2\beta^2 p_1 \cdot p_2 (p_{11}p_{12}p_{13}p_{21}p_{22}p_{23})} \frac{\mathcal{H}_{\text{num}}}{\mathcal{H}_{\text{den}}} \quad (\text{B2})$$

and

$$\mathcal{H}_{\text{num}} = 2c_\theta^2 m_Z^2 (\Gamma_Z^2 + m_Z^2) - (4c_\theta^2 + 3) m_Z^2 (p_1 \cdot p_2) + 6(p_1 \cdot p_2)^2, \quad (\text{B3a})$$

$$\mathcal{H}_{\text{den}} = m_Z^4 + \Gamma_Z^2 m_Z^2 - 4m_Z^2 (p_1 \cdot p_2) + 4(p_1 \cdot p_2)^2. \quad (\text{B3b})$$

The coefficients in eq. (B1) are given by

$$H_0 = 2p_{22} \left[(p_{11})^2 \left[(p_{13})^3 p_{21} p_{22} + p_{12} (p_{23})^2 (p_{21} q_{23} + p_{22} p_{23}) - p_{12} p_{13} p_{23} (p_{12} p_{21} + p_{21} (q_{23} - 2p_{23}) + p_{22} (p_{23} - q_{13})) \right] - p_{11} p_{12} p_{13} p_{21} p_{23} (p_{21} q_{23} + p_{22} p_{23}) - (p_{12})^2 (p_{13})^2 (p_{21})^2 p_{23} \right], \quad (\text{B4a})$$

$$H_1 = -p_{22} \left\{ 2p_{12} p_{13} (p_{21})^2 p_{22} q_{13} + (p_{11})^2 p_{23} \left[2(p_{12})^2 (p_{23} + q_{13}) + p_{12} (p_{13} (p_{21} + p_{22}) - 2p_{21} q_{23}) + p_{13} p_{21} p_{22} \right] + p_{11} p_{21} \left[2(p_{13})^2 p_{21} p_{22} + p_{12} p_{13} (2(p_{23} q_{12} + q_{13} q_{23}) + p_{21} (p_{23} - 2q_{23})) + 2p_{12} p_{23} q_{13} q_{23} \right] \right\}, \quad (\text{B4b})$$

$$H_2 = p_{11} p_{21} \left[p_{13} p_{22} (2p_{11} q_{23} + p_{23} q_{12}) + p_{12} p_{23} (p_{13} q_{12} + 2p_{21} q_{23}) \right]. \quad (\text{B4c})$$

Finally, the purely non-linear amplitude is given by

$$\langle |\mathcal{M}_Y|^2 \rangle = \mathcal{J} \left[\sum_{n=0}^3 (p_1 \cdot p_2)^n J_n + \text{perm.} \right] \quad (\text{B5})$$

where

$$\mathcal{J} = \frac{c_\theta^4 e^2}{2\beta^4 (p_1 \cdot p_2)^2} \frac{\mathcal{J}_{\text{num}}}{\mathcal{J}_{\text{den}}}, \quad (\text{B6})$$

with

$$\mathcal{J}_{\text{num}} = 2c_\theta^4 m_Z^2 (\Gamma_Z^2 + m_Z^2) - 6c_\theta^2 m_Z^2 (p_1 \cdot p_2) + 5(p_1 \cdot p_2)^2, \quad (\text{B7a})$$

$$\mathcal{J}_{\text{den}} = m_Z^4 + \Gamma_Z^2 m_Z^2 - 4m_Z^2 (p_1 \cdot p_2) + 4(p_1 \cdot p_2)^2. \quad (\text{B7b})$$

The coefficients in eq. (B5) are given by

$$J_0 = 3(p_{11})^2 p_{22} p_{23} q_{23} - 6p_{11} p_{12} p_{22} p_{23} q_{13} + 3p_{12} p_{13} (p_{21})^2 q_{23}, \quad (\text{B8a})$$

$$J_1 = 3p_{11} q_{23} (p_{21} q_{23} - 2p_{22} q_{13}) + (p_{11})^2 (q_{23})^2 + (p_{21})^2 (q_{23})^2, \quad (\text{B8b})$$

$$J_2 = q_{12} q_{13} q_{23}. \quad (\text{B8c})$$

-
- [1] O. Halpern, *Scattering processes produced by electrons in negative-energy states*, Phys. Rev. **44**, 855 (1933).
[2] M. Born, L. Infeld, *Foundations of the new field theory*, Nature **132**, 1004 (1933).
[3] W. Heisenberg, H. Euler, *Consequences of Dirac's theory of positrons*, Zeit. Phys. **98** 714 (1936).
[4] S. I. Kruglov, *Born-Infeld-type electrodynamics and magnetic black holes*, Annals of Physics **383**, 550 (2017).
[5] S. I. Kruglov, *Gravitation and Cosmology, Dyonic Black Holes with Nonlinear Logarithmic Electrodynamics*, **25** 190 (2019).
[6] N. Bretón, *Nonlinear electrodynamics and cosmology*, J. Phys. Conf. Ser. **229** 012006 (2010).
[7] R. García-Salcedo, N. Bretón, *Born-Infeld Cosmologies*, Int. J. Mod. Phys. A **15** 4341 (2000).
[8] P. Gaete, J.A. Helayël-Neto, *Finite field-energy and interparticle potential in logarithmic electrodynamics*, Eur.Phys.J.C **74** 3, 2816 (2014).
[9] P. Gaete, J. A. Helayël-Neto, *Remarks on nonlinear electrodynamics*, Eur. Phys. J. C **74**, 3182 (2014).
[10] P. Gaete, J. A. Helayël-Neto, *A note on nonlinear electrodynamics*, EPL **119**, 51001 (2017).
[11] M. J. Neves, J. B. de Oliveira, L. P. R. Ospedal, J. A. Helayël-Neto, *Dispersion Relations in Non-Linear Electrodynamics and the Kinematics of the Compton Effect in a Magnetic Background*, Phys. Rev. D **104**, 015006 (2021).
[12] I. Gullu, S. H. Mazharimousavi, *Double-logarithmic nonlinear electrodynamics*, Phys. Scr. **96** 045217 (2021).
[13] I. Bandos, K. Lechner, D. Sorokin and P. K. Townsend, *Nonlinear duality-invariant conformal extension of Maxwell's equations*, Phys. Rev. D **102**, 121703(R) (2020).
[14] ATLAS Collaboration, *Evidence for light-by-light scattering in heavy-ion collisions with the ATLAS detector at the LHC*, Nature Physics **13**, 852 (2017).
[15] ATLAS Collaboration, *Observation of Light-by-Light Scattering in Ultrapерipheral Pb + Pb Collisions with the ATLAS Detector*, Phys. Rev. Lett. **123**, 052001 (2019).
[16] P.A.M. Dirac, *Quantised singularities in the electromagnetic field*, Proc. R. Soc. Lond. A **133**, 60-72 (1931).
[17] Y.M. Cho, D. Maison, *Monopoles in Weinberg-Salam*

- Model*, Phys. Lett. B **391**, 360 (1997).
- [18] Y. M. Cho, K. Kim, J. H. Yoon, *Finite energy electroweak dyon*, Eur. Phys. J. C **75**, 67 (2015).
- [19] J. Ellis, N. E. Mavromatos, T. You, *The Price of an Electroweak Monopole*, Phys. Lett. B **756**, 29 (2016).
- [20] P. Zhang, L. Zou, Y. M. Cho, *Regularization of Electroweak Monopole by Charge Screening and BPS Energy Bound*, Eur. Phys. J. C **80**, 280 (2020).
- [21] S. Arunasalam, A. Kobakhidze, *Electroweak monopoles and the electroweak phase transition*, Eur. Phys. J. C **77**, no. 7, 444 (2017).
- [22] P. De Fabritiis, J.A. Helayël-Neto, *Electroweak monopoles with a non-linearly realized weak hypercharge*, Eur. Phys. J. C **81**, 788 (2021).
- [23] B. Acharya *et al* (MoEDAL Collaboration), *The physics programme of the MoEDAL experiment at the LHC*, Int. J. Mod. Phys. A **29**, 1430050 (2014).
- [24] P. Niau Akmansoy, L. G. Medeiros, *Constraining Born-Infeld-like nonlinear electrodynamics using hydrogen's ionization energy*, Eur. Phys. J. C **78**, 143 (2018).
- [25] M. Fouché, R. Battesti, C. Rizzo, *Limits on nonlinear electrodynamics*, Phys. Rev. D **93**, 093020 (2016).
- [26] J. Ellis, N. E. Mavromatos and T. You, *Light-by-Light Scattering Constraint on Born-Infeld Theory*, Phys. Rev. Lett. **118**, 261802 (2017).
- [27] E. S. Fradkin, A. A. Tseytlin, *Non-linear electrodynamics from quantized strings*, Phys. Lett. B **163**, 123 (1985).
- [28] C. G. Callan, J. M. Maldacena, *Brane dynamics from the Born-Infeld action*, Nucl. Phys. B **513**, 19 (1998).
- [29] S. Godfrey, *Quartic gauge boson couplings*, AIP Conf. Proc. 350, 41 (1995), arXiv:hep-ph/9505252.
- [30] A. Barroso, F. Boudjema, J. Cole, N. Dombey, *Electromagnetic properties of the Z boson. I*, Z. Phys. C **28**, 149 (1985).
- [31] J. Ellison, J. Wudka, *Study of trilinear gauge boson couplings at the Tevatron collider*, Annu. Rev. Nucl. Part. Sci. **48**, 33 (1998).
- [32] M. Baillargeon, F. Boudjema, *Contribution of the bosonic loops to the three photon decay of the Z*, Phys. Lett. B **272**, 158 (1991).
- [33] X. Pham, *Non-Abelian effects in nonlinear quantum electrodynamics and in Z0 decay into three photons*, Phys. Lett. B **272**, 373 (1991).
- [34] E. W. N. Glover, A. G. Morgan, *Z boson decay into photons*, Z. Phys. C **60**, 175 (1993).
- [35] P.A. Zyla *et al.*, *Particle Data Group*, Prog. Theor. Exp. Phys. **2020**, 083C01 (2020) and 2021 update.
- [36] ATLAS Collaboration, *Search for new phenomena in events with at least three photons collected in pp collisions at $\sqrt{s} = 8$ TeV with the ATLAS detector*, Eur. Phys. J. C **76**, 210 (2016).
- [37] L3 Collaboration, *Search for anomalous $Z \rightarrow \gamma\gamma\gamma$ events at LEP*, Phys. Lett. B **345**, 609 (1995).
- [38] S. Villa, *Gauge boson couplings at LEP*, Nucl. Phys. B **142**, 391 (2005).
- [39] M. A. Perez, G. Tavares-Velasco, J. J. Toscano, *New physics effects in rare Z decays*, Int. J. Mod. Phys. A **19**, 159 (2004).
- [40] M. Stohr, J. Horejsi, *Effective lagrangians for the Z boson decay into photons*, Phys. Rev. D **49**, 3775 (1994).
- [41] M. J. Neves, L.P.R. Ospedal, J.A. Helayël-Neto, Patricio Gaete, *Considerations on anomalous photon and Z-boson self-couplings from the Born-Infeld weak hypercharge action*, arXiv:hep-th/2109.11004.
- [42] K. Buesser, *The International Linear Collider*, arXiv:physics.acc-ph/1306.3126.
- [43] D.M. Asner *et al.*, *ILC Higgs White Paper*, arXiv:hep-ph/1310.0763v4.
- [44] K. Fujii *et al.*, *ILC study questions for snowmass 2021*, arXiv:hep-ph/2007.03650v3.
- [45] K. Fujii *et al.*, *Tests of the Standard Model at the International Linear Collider*, arXiv:hep-ex/1908.11299.
- [46] A. Blondel, P. Janot, *FCC-ee overview: new opportunities create new challenges*, arXiv:hep-ex/2106.13885.
- [47] P. Azzurri, G. Bernardi, S. Braibant, D. d'Enterria, J. Eysermans, P. Janot, A. Li, E. Perez, *A special Higgs challenge: Measuring the mass and production cross section with ultimate precision at FCC-ee*, arXiv:hep-ex/2106.15438.
- [48] W. de Boer, *Precision experiments at LEP*, Adv. Ser. Direct. High Energy Phys. **23**, 107 (2015).
- [49] T. Lesiak *Future e^+e^- colliders at the energy frontier*, EPJ Web Conf. **206**, 08001 (2019).
- [50] CEPC-SPPC Study Group, *Electroweak physics at CEPC*, PoS ICHEP **2016**, 692 (2016).
- [51] Aicheler, M. *et al.* (eds.), *The Compact Linear Collider (CLIC) - Project Implementation Plan*, CERN, 2018, arXiv:physics.acc-ph/1903.08655.
- [52] L3 Collaboration, *A test of electrodynamics in the reaction $e^+e^- \rightarrow \gamma\gamma(\gamma)$* , Phys. Lett. B **288**, 404 (1992).
- [53] L3 Collaboration, *Study of multiphoton final states and tests of QED in e^+e^- collisions at \sqrt{s} up to 209 GeV*, Phys. Lett. B **531**, 28 (2002).
- [54] F.A. Berends, R. Kleiss, *Distributions for electron-positron annihilation into two and three photons*, Nucl. Phys. B **186**, 22 (1981).
- [55] A.F. Zarnecki, *On the physics potential of ILC and CLIC*, arXiv:hep-ph/2004.14628.
- [56] B. Badelek *et al.*, *TESLA Technical Design Report, Part VI, Chapter 1: The Photon Collider at TESLA*, Int. J. Mod. Phys. A **19**, 5097 (2004).
- [57] R. Appleby, P. Bambade, *Photon production at the interaction point of the ILC*, arXiv:physics.acc-ph/0803.3519.
- [58] Kwang-Je Kim, *Gamma gamma collider based on Compton back scattering*, Nucl. Instrum. Meth. A **393**, 530 (1997).
- [59] V. I. Telnov, *Principles of photon colliders*, Nucl. Instrum. Meth. A **355**, 3 (1995).
- [60] A. Denner, S. Dittmaier, R. Schuster, *Radiative corrections to $\gamma\gamma \rightarrow W^+W^-$ in the electroweak Standard Model*, Nucl. Phys. B **452**, 80 (1995).
- [61] A. Denner, S. Dittmaier, R. Schuster, *Electroweak radiative corrections to $\gamma\gamma \rightarrow W^+W^-$* , arXiv:hep-ph/9601355.
- [62] E. Yehudai, *Probing W gamma couplings using $\gamma\gamma \rightarrow W^+W^-$* , Phys. Rev. D **44**, 3434 (1991).
- [63] L. Meitner, H. Kötters (and M. Delbruck), *Ueber die streuung kurzwelliger γ -strahlen*, Z. Phys. **84**, 137 (1933).
- [64] B. De Tollis, *The scattering of photons by photons*, Nuovo Cim. **35**, 1182 (1965).
- [65] D.A. Dicus, C. Kao, *Production of Z boson pairs at photon linear colliders*, Phys. Rev. D **49**, 1265 (1994).
- [66] G.V. Jikia, *Z boson pair production in high energy photon-photon collisions and the Higgs signal*, Phys. Lett. B **298**, 224 (1993).
- [67] C. Fleper, W. Kilian, J. Reuter *et al.*, *Scattering of W and Z bosons at high-energy lepton colliders*, Eur. Phys. J. C **77**, 120 (2017).